Kinematic Synthesis for Smart Hand Prosthesis

Karthikeyan Duraisamy, Obiajulu Isebor and Alba Perez*
Measurement and Controls Engineering Research Center (MCERC)
College of Engineering
Idaho State University
833 South 8th Ave., Pocatello, ID 83209, USA
{*durakart,isebobia,perealba*}*@isu.edu*

Marco P. Schoen and D. Subbaram Naidu
Measurement and Controls Engineering Research Center (MCERC)
College of Engineering
Idaho State University
833 South 8th Ave., Pocatello, ID 83209, USA
{*schomarc,naiduds*}*@isu.edu*

***Abstract*— The dream of a bionic replacement appendage is becoming reality through the use of mechatronic prostheses that utilize the body's myoelectric signals. This paper presents a process to accurately capture the motion of the human hand joints; the obtained information is to be used in conjunction with myoelectric signal identification for motion control.**

In this work, the human hand is modeled as a set of links connected by joints, which are approximated to standard revolute joints. Using the methods of robotics, the motion of each finger is described as a serial robot, and expressed as Clifford algebra exponentials. This representation allows us to use the model to perform kinematic synthesis, that is, to adapt the model to the dimensions of real hands and to obtain the angles at each joint, using visual data from real motion captured with several cameras.

The goal is to obtain an adaptable motion tracking system that can follow as many different motions as possible with sufficient accuracy, in order to relate the individual motions to myoelectric signals in future work.

***Index Terms*— Artificial hands, Biomechanical modeling, EMG-based interfaces, Prostheses control systems, Models of animal/human manipulation.**

I. Introduction

Upper-body prosthetic devices have seen little improvement in terms of functionality and ability since World War II. This is in contrast to the large demand for advanced artificial hands and arms in recent years due to the involvement of military forces on various battle-fields. While better body armor has been effective in saving lives and reducing the fatalities overall, these protective devices leave the extremities of the body unshielded and hence the rise in the number of amputations for combat troops. While the development for leg and foot prosthetic devices has enjoyed much attention due to the higher number of incidents such as foot amputation due to diabetic neuropathy hand prosthetics lack in availability and functionality. Research in developing smart or intelligent artificial hands has been conducted primarily by the movie industry, for creating special effects or controlling robotic devices via a human interface. Interest by NASA to teleoperate devices in space resulted in research pertaining myoelectric signals.

Myoelectric signal is the term given to the nerve impulse that travels from the brain to a muscle and initiates action. Even though an individual's appendage is gone, the body is still able to convey the nerve impulses that excited the muscles of the missing appendage. Myoelectric signals are built up of nerve impulses, which are a chain of ionic chemical reactions. Due to the ion exchange of the neurons, a potential difference is built up and can be measured as an electrical voltage [1]. The voltage is significant enough that myoelectric signals can be collected directly from the skin in a non-invasive way. By intercepting these myoelectric signals before they reach the missing appendage it is possible to activate a prosthesis that acts as the original appendage would. This gives the wearer some control of the prosthesis.

Currently there are several myoelectric prostheses for individual use all at varying cost and level of control; however, there are no prostheses that fully simulate the intricacies of the human hand. In part this is due to the complexity of the prosthesis required to simulate the human hand, but also the complexity of the controller required to interpret the myoelectric signals. Myoelectric signals continually change their pattern and strength complicating the implementation of myoelectric prostheses.

Current technology for decoding myoelectric signals is focused on essentially pattern recognizing methods utilizing neural networks and genetic algorithms that approximate the signals [2]. These methods require "training" of the prosthesis and are in themselves complex, which leads to large, slow models of the myoelectric signals.

Previous work by some of the authors has been focusing on using system identification, effectively treating the myoelectric signal source as a dynamic system [4]. The system identification experiment yields mathematical models, which predict the intended motion of the missing hand. This approach has the advantage of taking into account the adaptive nature of the necessary control scheme in order to counter fatigue, while increasing the implementation time and hence reducing the computations required to interpret the myoelectric signals.

Previous results indicate the need of a complete hand kinematics model, to simulate an artificial hand and to correlate the myoelectric signals to hand motion with a high degree of precision and detail, in order to decide which muscle group and its associated motion have to be investigated and/or identified.

The presented material in this paper is a building block

*Corresponding author

for the development of an artificial hand controlled using myoelectric signals. It addresses the development of a detailed kinematic model representing the human hand, as well as the procedure to identify the motion of each joint of the hand.

II. The Human Hand

Hand and wrist are some of the unique parts of the upper extremity. The skeleton of the hand consists of 27 bones. Eight of them are carpal bones, organized in two rows of proximal (movable) and distal (immovable) carpal bones. The other 19 are long bones, which extend in five rays (polyarticulated serial chains) made of metacarpal bones and phalanges (proximal, middle and distal). The wrist consists of the radial and ulna bones.

Joints are formed at the surface of relative motion between two bones. For some of the joints, their motion can be approximated to that of a revolute joint, even though the real motion is more complicated and requires the model of the matching surfaces. Some other joints can perform motion in different directions and can be modeled as two-degree-of-freedom joints.

The joints considered are: radio-ulna joint at the wrist, midcarpal joint between the proximal and distal carpal joint, carpo-metacarpal (CMC) joint between distal carpal row and the metacarpal bone, metacarpal-phalangeal joint (MCP) between metacarpal and proximal phalange bone, and proximal and distal phalangeal joints separating the phalangeal bones.

The range of motion of each joint and the dimensions and type of joints for our simulations were taken from several sources [5], [7], [6] that present some variability in their numerical values.

A. Wrist and Carpal Motion

The wrist movement comprises flexion/extension and adduction/abduction, and also a certain degree of circular movement that we will neglect. The rotation about the lower arm will comprise most of the motion about that direction. In addition we include here the motion between the two carpal rows, that can be assumed to rotate about their border as units. This is a total of three degrees of freedom that are common to all fingers.

B. Index and Middle Fingers

Both the index and middle finger rays have a similar motion. They have flexion, extension and certain degree of abduction and adduction at the MCP joint. There is negligible movement at the CMC joints, which in turn gives these two rays four degrees of freedom for each.

C. Ring and Little Fingers

The ring and the little fingers are also called the ulna digits. They have the same features as the index and middle finger, but they have greater mobility at the CMC joint, which cannot be neglected. This gives five degrees of freedom to each of them.

D. Thumb Finger

The thumb has greater mobility when compared to the other fingers, and its joints present a more complex motion. The bones that are responsible for thumb movement are: scaphoid, trapezium, first metacarpal, proximal and distal phalanges. All these bones give a total of five degrees of freedom to the thumb. The CMC joint is a biaxial joint (sellar/saddle joint) that performs flexion/extension and adduction/abduction. The MCP joint is a condyloid joint (biaxial joint). There is flexion/extension, adduction/abduction and slight rotation that we can neglect. The distal phalangeal joint is a hinge joint more similar to those of the other fingers, that presents one degree of freedom.

III. Kinematic Modeling of the Human Hand

A. Introduction

A kinematic model of the human hand has been developed in order to track independently the motion in each degree of freedom. We model each of the fingers as a serial kinematic chain composed of revolute joints. We include the motion (abduction/ adduction and flexion / extension) of the wrist and future models will include the pronation/supination rotation about the radius-ulna direction, because they greatly contribute to the manipulation and grasping motion of the hand.

Most of the actual motion tracking models represent the joints as a spherical joint, that is, an arbitrary rotation matrix located at a point. Even though this modeling gives fast results, it does not capture the actual structure of the skeleton so precisely, where the rubbing surfaces create joints with well-defined joint axes in many cases. It also increases the number of parameters to track. A different type of research [8] is directed to describe in detail the rubbing surfaces of the bones, obtaining a very detailed description of the joint motion. Unlike these two approaches, we model the joints as revolute or universal joints. This allows us to have a precise description of the motion with less joint parameters, as well as to have a more defined description of the kinematics structure, without a very high computational load.

We use Clifford algebra exponentials to represent the motion at each joint, expressed as relative motion from an initial, or reference, configuration. The complete motion is obtained by composing the motion about each joint, using the Clifford algebra product.

In order to be able to properly track the motion of the subject, we need to adapt the dimensions and morphology of the generic hand model to that of the individual being studied. For doing that, we use the visual data to perform first kinematic synthesis plus inverse kinematics. Once the model of the hand is adapted to that of the individual, only the inverse kinematics, or motion tracking, is needed.

B. The Kinematics Equations of a Serial Chain

The kinematics equations for a serial chain define the position of its end-effector as a function of the geometry of the chain and the joint variables. They can be expressed

as a product of local displacements using the Denavit-Hartenberg parameters. Consider the serial chain defined by several joint axes S_i as in Fig. 1.

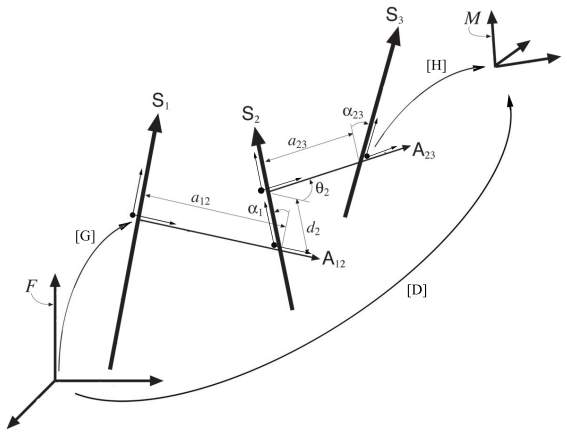

Fig. 1. Generic serial chain with m joints.

For the m-jointed kinematic chain, the kinematics equations, expressed as homogeneous transformations, are

$$\begin{aligned}[D_i] =&[G][Z(\theta_1^i, d_1^i)][X(\alpha_{12}, a_{12})][Z(\theta_2^i, d_2^i)]\dots \\ &[X(\alpha_{n-1,n}, a_{n-1,n})][Z(\theta_m^i, d_m^i)][H], \quad i = 1, \dots n,\end{aligned} \tag{1}$$

where $[G]$ locates the base of the chain with respect to the fixed reference frame F, and $[H]$ represents the displacement between the end-effector and the last joint m.

We do not use this version of the kinematics equations but rather the equations defining relative motion with respect to a reference configuration $[D_0]$, given by $[D_{0i}] = [D_i][D_0]^{-1}$. These take the form

$$[D_{0i}(\Delta\vec{\theta^i})] = [T(\Delta\theta_1^i, \mathsf{S}_1)][T(\Delta\theta_2^i, \mathsf{S}_2)]\dots[T(\Delta\theta_m^i, \mathsf{S}_m)]. \tag{2}$$

The matrices $[T(\Delta\theta_j^i, \mathsf{S}_j)]$ represent screw displacements about the joint axes S_j. These are expressed in the fixed frame and at the reference configuration using Plücker coordinates , $\mathsf{S}_j = \mathbf{S}_j + \epsilon\mathbf{S}_j^0$, and $\Delta\theta_j^i = \theta_j^i - \theta_j^0$ is the joint variable j measured from the reference configuration.

C. Clifford Algebra Kinematics Equations

The Clifford algebra of the projective three-space $\mathbb{P}^3$ is a sixteen-dimensional vector space with a non-commutative product called geometric or Clifford product [14]. The elements of even rank form an eight-dimensional subalgebra $C^+(\mathbb{P}^3)$ that can be identified with the set of 4×4 homogeneous transforms.

In our calculations, we use the notation $\mathbf{s} = s_1 i + s_2 j + s_3 k$ and $\mathbf{s}^\circ = s_5 i + s_6 j + s_7 k$, so that we write the Clifford algebra element as

$$\hat{S} = s_0 + \mathbf{s} + s_4\epsilon + \mathbf{s}^\circ\epsilon = (s_0 + s_4\epsilon) + (\mathbf{s} + \mathbf{s}^\circ\epsilon) = \hat{s} + \mathsf{S}. \tag{3}$$

For more information about the Clifford algebra of dual quaternions used in kinematic synthesis, see [13].

A spatial displacement is identified with the unit dual quaternion obtained as the Clifford algebra exponential of the screw $\mathsf{J} = \mathbf{s} + \epsilon(\mathbf{c} \times \mathbf{s} + \mu\mathbf{s})$

$$\hat{Q} = e^{\frac{\hat{\phi}}{2}\mathsf{J}} = \cos\frac{\hat{\phi}}{2} + \sin\frac{\hat{\phi}}{2}\mathsf{S}, \tag{4}$$

where $\mathsf{S} = \mathbf{s} + \epsilon(\mathbf{c} \times \mathbf{s})$ is the screw axis of the displacement, and $\hat{\phi}$ is the dual axis variable defined as $\hat{\phi} = \phi + \epsilon t$, where t is the translation along and ϕ is the rotation about the axis.

The composition of these Clifford algebra elements defines the relative kinematics equations for a serial chain that are equivalent to Eq. (2) as the product of Clifford algebra exponentials,

$$\begin{aligned}\hat{D}_i(\Delta\hat{\vec{\theta}}) =&\hat{Q}_1(\hat{\theta}_1^i)\hat{Q}_2(\hat{\theta}_2^i)\dots\hat{Q}_m(\hat{\theta}_m^i) \\ =&e^{\frac{\Delta\hat{\theta}_{1j}}{2}\mathsf{S}_1}e^{\frac{\Delta\hat{\theta}_{2j}}{2}\mathsf{S}_2}\dots e^{\frac{\Delta\hat{\theta}_{nj}}{2}\mathsf{S}_m},\end{aligned} \tag{5}$$

where $\hat{Q}_j(\hat{\theta}_j^i) = \cos\frac{\Delta\hat{\theta}_j^i}{2} + \sin\frac{\Delta\hat{\theta}_j^i}{2}\mathsf{S}_j$ corresponds to the relative transformation of the chain about joint j from the reference configuration $\hat{D}_0$.

D. The Hand Model

The hand is modeled as five independent serial chains with eight degrees of freedom each, corresponding to the five fingers. The first three joints, corresponding to the flexion/extension and abduction/adduction of the radio-ulnar joint at the wrist, and the carpal joint between proximal and distal carpal row, are common to all five chains. From there on, the carpo-metacarpal joint is modeled as a revolute joint; the metacarpo-phalangeal joint is modeled as two revolute joints intersecting at 90 degrees; and the proximal and distal phalangeal joints are modeled as revolute joints.

The kinematics equations, as relative motion from a reference configuration, are given by

$$\begin{aligned}\hat{Q}_{index} =&\hat{S}_{c1}(\theta_1)\hat{S}_{c2}(\theta_2)\hat{S}_{c3}(\theta_3)\hat{S}_{i4}(\theta_4)\dots\hat{S}_{i7}(\theta_7)\hat{S}_{i8}(\theta_8) \\ =&(\cos\frac{\theta_1}{2} + \sin\frac{\theta_1}{2}\mathsf{S}_{c1})(\cos\frac{\theta_2}{2} + \sin\frac{\theta_2}{2}\mathsf{S}_{c2})\dots \\ &(\cos\frac{\theta_8}{2} + \sin\frac{\theta_8}{2}\mathsf{S}_{i8}).\end{aligned} \tag{6}$$

This corresponds to the axes shown in Fig. 2 for the reference configuration.

A rotation about a revolute joint $\mathsf{S} = \mathbf{s} + \epsilon\mathbf{s}^0$ takes the form, if we write the scalar as the fourth component of the vector,

$$\hat{S}(\theta) = \cos\frac{\theta}{2} + \sin\frac{\theta}{2}\mathsf{S} = \begin{Bmatrix}\sin\frac{\theta}{2}s_x \\ \sin\frac{\theta}{2}s_y \\ \sin\frac{\theta}{2}s_z \\ \cos\frac{\theta}{2}\end{Bmatrix} + \epsilon\begin{Bmatrix}\sin\frac{\theta}{2}s_x^0 \\ \sin\frac{\theta}{2}s_y^0 \\ \sin\frac{\theta}{2}s_z^0 \\ 0\end{Bmatrix}.$$

The dual quaternion expression of two revolute joints $\mathsf{S}_1 = \mathbf{s}_1 + \epsilon(\mathbf{c} \times \mathbf{s}_1)$ and $\mathsf{S}_2 = \mathbf{s}_2 + \epsilon(\mathbf{c} \times \mathbf{s}_2)$ intersecting

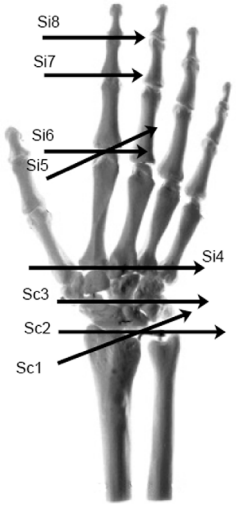

Fig. 2. Kinematic model for the index finger. (Illustration from Authentic anatomical^{TM} model)

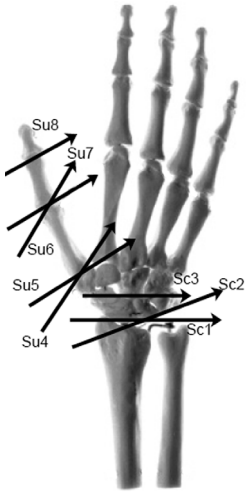

Fig. 3. Kinematic model for the thumb finger

at a right angle at point $\mathbf{c}$ is somewhat simpler than the product of two general rotations; we denote it by $\hat{T}$,

$$\hat{T}_{12}(\theta_1,\theta_2) = (\cos\frac{\theta_1}{2} + \sin\frac{\theta_1}{2}\mathsf{S}_1)(\cos\frac{\theta_2}{2} + \sin\frac{\theta_2}{2}\mathsf{S}_2) = \begin{Bmatrix} \mathbf{s}_1 s\frac{\theta_1}{2}c\frac{\theta_2}{2} + \mathbf{s}_2 c\frac{\theta_1}{2}s\frac{\theta_2}{2} + \mathbf{s}_1\times\mathbf{s}_2 s\frac{\theta_1}{2}s\frac{\theta_2}{2} \\ c\frac{\theta_1}{2}c\frac{\theta_2}{2} \end{Bmatrix} + \epsilon\begin{Bmatrix} \mathbf{c}\times\left(\mathbf{s}_1 s\frac{\theta_1}{2}c\frac{\theta_2}{2} + \mathbf{s}_2 c\frac{\theta_1}{2}s\frac{\theta_2}{2} + (\mathbf{s}_1\times\mathbf{s}_2)s\frac{\theta_1}{2}s\frac{\theta_2}{2}\right) \\ 0 \end{Bmatrix}. \tag{7}$$

In addition, for the index finger the motion at the carpo-metacarpal joint (S_4) is negligible. Considering this, the kinematics equations for the index finger are written as

$$\hat{Q}_{index} = \hat{T}_{c12}(\theta_1,\theta_2)\hat{S}_{c3}(\theta_3)\hat{T}_{i56}(\theta_5,\theta_6)\hat{S}_{i7}(\theta_7)\hat{S}_{i8}(\theta_8). \tag{8}$$

The kinematics equations for the middle, third and fourth finger present the same structure; the motion of the carpo-metacarpal joint is also negligible for the middle finger, but not for the third and fourth finger,

$$\begin{aligned} \hat{Q}_{mid} =& \hat{T}_{c12}(\theta_1,\theta_2)\hat{S}_{c3}(\theta_3)\hat{T}_{m56}(\theta_5,\theta_6)\hat{S}_{m7}(\theta_7)\hat{S}_{m8}(\theta_8), \\ \hat{Q}_{third} =& \hat{T}_{c12}(\theta_1,\theta_2)\hat{S}_{c3}(\theta_3)\hat{S}_{t4}(\theta_4)\hat{T}_{t56}(\theta_5,\theta_6)\hat{S}_{t7}(\theta_7) \\ & \hat{S}_{t8}(\theta_8), \\ \hat{Q}_{four} =& \hat{T}_{c12}(\theta_1,\theta_2)\hat{S}_{c3}(\theta_3)\hat{S}_{f4}(\theta_4)\hat{T}_{f56}(\theta_5,\theta_6)\hat{S}_{f7}(\theta_7) \\ & \hat{S}_{f8}(\theta_8). \end{aligned} \tag{9}$$

The thumb is modeled so that the carpo-metacarpal joint consists of two intersecting revolute joints, same as the metacarpo-phalangeal joint. There is only one phalangeal joint, modeled as a revolute joint; see Fig. 3.

To verify the kinematic model, the standard dimensions are introduced in the model and a series of linear joint trajectories are generated. Some snapshots of the resulting motion of the hand are shown in Fig. 4. This model is considered an appropriate good approximation that provides a good description of the motion of the hand using a total of 26 joint parameters.

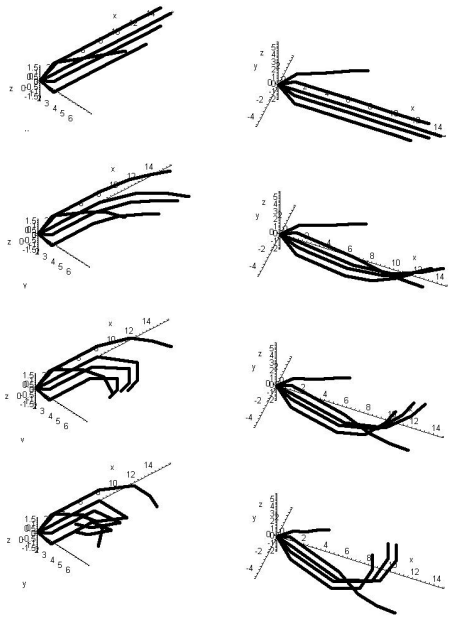

Fig. 4. Simulation of the hand using the forward kinematics model

IV. Kinematic Synthesis and Tracking for the Human Hand

A. Kinematic Synthesis

The kinematic synthesis for a serial chain defines the topology and dimensions of the chain that provides a desired motion of the end-effector. Dimensional synthesis assumes that the topology of the chain is specified and only its dimensions are to be determined for a specified motion. Several approaches to solve this problem have been developed; see for instance [9] or [10]. More recently, Lee and Mavroidis [11] used the matrix kinematics equations of the chain for a set of selected positions and solved for

the Denavit-Hartenberg parameters that satisfy these matrix equations. Our approach follows Perez and McCarthy [12], [13], who use a similar technique but using relative transformations and expressing the kinematics equations as Clifford algebra exponentials, known as dual quaternions.

The human skeleton presents a relatively high number of degrees of freedom. The dual quaternion approach provides with an efficient formulation of the design equations for these chains, which can be applied to the serial chains with any number of degrees of freedom.

B. Dimensional Synthesis Using Clifford Algebras

The goal of our synthesis problem is to determine the dimensions and angles of the serial chains that can perform the motion given by real hand data.

Consider that the real hand data are defined as finite displacements $[P_j]$, $j = 1, \ldots, m$. We choose $[P_1]$, the first frame, as the reference position and compute the relative displacements $[P_j][P_1^{-1}] = [P_{1j}]$, $j = 2, \ldots, n$ and express them as unit dual quaternions, $\hat{P}_{1j}$=cos $\frac{\hat{\phi}_{1j}}{2}$ + sin $\frac{\hat{\phi}_{1j}}{2}$ P_{1j}, $j = 2, \ldots, n$.

The solution of the dimensional synthesis problem is given by the values S_j and θ_j, $j = 1, \ldots, m$, such that the displacement performed by the serial chain is equal to the datum displacement $\hat{P}_{1j}$,

$$\hat{P}_{1j} = e^{\frac{\Delta\hat{\theta}_{1j}}{2}\mathsf{S}_1} e^{\frac{\Delta\hat{\theta}_{2j}}{2}\mathsf{S}_2} \cdots e^{\frac{\Delta\hat{\theta}_{nj}}{2}\mathsf{S}_n}, \quad j = 2, \ldots, n. \quad (10)$$

For m datum displacements, the result is $8(m-1)$ design equations. The unknowns are the m joint axes S_i, $i = 1, \ldots, m$, and the $m(n-1)$ pairs of joint parameters $\theta_{ij} + d_{ij}\epsilon$.

It is easy to see that these equations become complicated quickly. If we wanted to solve for a single finger considering only positions of the fingertip, we would have $8 \times 4 = 32$ design parameters and $8 \times (n-1)$ joint variables as unknowns; considering, in order to simplify the problem, that the motion of the last three joints is not independent, we would need 33 data positions in order to solve for 264 nonlinear equations.

One of the advantages of the structure of the Clifford algebra design equations is that it provides a systematic approach to assembling the design equations for any serial chain. The basic approach is to formulate the design equations for the general serial chain with screw displacements at each joint, and then restrict the resulting equations to a particular topology.

Visual data from real hand motion present also the advantage that we may have information not only about the motion of the tip of the fingers, but also about the intermediate links. This allows us to apply the synthesis hierarchically [15], simplifying the solution process.

C. Hierarchical Synthesis

We present here the procedure to solve for the serial chain of the index finger; the rest of the chains are solved similarly. The hierarchical synthesis process consists of solving sequentially link after link along the chain, starting from the base. We assume that we have data about the position of each differentiated link in the hand.

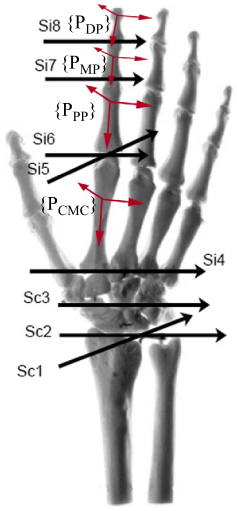

Fig. 5. Frames defining differentiated links along the index finger

As initial data, we consider that we can attach a reference frame to the following hand sections: we consider the lower arm as the base and assume that it is not moving. Then we have $\hat{P}_{CMC}$, $\hat{P}_{PP}$, $\hat{P}_{MP}$ and $\hat{P}_{DP}$ for position of the carpal and metacarpal area, proximal, middle and distal phalanges. We do not consider likely that we will be able to separate the motion of the carpal and the metacarpal areas, so we consider them as a unit data here; see Fig. 5.

The first step of the process consists of solving for the first joints of (8),

$$\hat{T}_{c12}(\theta_1^i, \theta_2^i)\hat{S}_{c3}(\theta_3^i) = \hat{P}_{CMC}^i, \quad i = 2, \ldots n, \quad (11)$$

so that they can perform the motion captured in $\hat{P}_{CMC}$. To fully establish the dimensions of the first three joints, $n = 5$ different positions are needed.

Once those are determined, we can solve for the next joint using the calculated result, which we denote , $\tilde{Q}_{123}$, so that

$$\hat{T}_{i56}(\theta_5^i, \theta_6^i) = (\tilde{Q}_{123}^i)^* \hat{P}_{PP}^i, \quad i = 2, 3, \quad (12)$$

where $*$ denotes the conjugate, or inverse, dual quaternion. To solve for the carpo-metacarpal joint, at least $n = 3$ positions are needed. We use the approximate solution to solve sequentially for the next two phalangeal joints,

$$\begin{aligned} \hat{S}_{i7}(\theta_7^i) &= (\tilde{Q}_{56}^i)^* (\tilde{Q}_{123}^i)^* \hat{P}_{MP}^i, \\ \hat{S}_{i8}(\theta_8) &= (\tilde{Q}_7^i)^* (\tilde{Q}_{56}^i)^* (\tilde{Q}_{123}^i)^* \hat{P}_{DP}^i. \end{aligned} \quad (13)$$

Each of these equations, can be solved quickly when solved separately. The solution process is repeated for several datasets and the solutions averaged to find the best approximation for the hand skeleton. The repeated solving process and averaging are necessary because of the lack of accuracy of the input data and of the rigid body model.

D. Future Work: Experimental Setup and Solving Process

The experimental setup has not been tested yet; the model is now in the process of being tested with synthetically generated data. However, a similar setup that we expect to replicate has been successfully applied by some of the authors for identifying skeleton dimensions in [15].

The motion of the hand will be captured by a set of at least four calibrated cameras. Several markers in the hand will be used as points to track and intersect in order to obtain their three-dimensional position. Those points will be used to create the frame attached to the different links of the hand. During the motion, we will obtain a series of finite displacements for each link, that we call frames, whose temporal separation depends on the speed of the cameras.

The subject will be asked to move the hand, which will be fixed to the base at the lower arm, while the cameras are recording the motion. This motion may be sub-sampled if needed. The recorded string of frames will be the input for the synthesis process. The synthesis process will be divided in two stages: at the first stage, the frames will be used to adapt the length and angles of the joints to the hand of the recorded subject. Once the skeleton is completed, the frames will be used to solve for the angles at the joints only, assuming that the location and orientation of the joints is close enough to the actual joints of the subject.

The equations are solved using a numeric algorithm that minimizes the distance between both dual quaternions, considering them as eight-dimensional vectors. The solver used in previous experiments of the same type is a Levenberg-Marquardt algorithm.

V. Conclusions

This paper presents a process to accurately capture the motion of the human hand joints. The joints are modeled as standard revolute joints and, using the methods of robotics, the motion of each finger is described as a serial robot, expressed as Clifford algebra exponentials. This representation allows us to use the model to perform kinematic synthesis, that is, to adapt it to the dimensions of real hands and to obtain the angles at each joint from visual data captured with several cameras. It is important to remark here that the kinematic model so obtained does not mimic the geometry of the hand, but rather its motion. Depending on the accuracy of the model, the geometry of the hand will be more or less accurately represented.

This method of motion identification is to be used as the input for the system identification of myoelectric signals from the human arm. The experimental implementation is being developed; the final goal is to identify and separate as many hand movements as possible, in order to create a hand prosthesis with a complex, human-like motion.

References

[1] R. Northrop, *Analysis and Application of Analog Electronic Circuits to Biomedical Instrumentation*, CRC Press, Boca Raton, Florida, 2004.

[2] M. Korenberg, and E. Morin, "Automatic Discrimination of Myoelectric Signals via Parallel Cascade Identification", Annals of Biomedical Engineering, Vol. 25, pp. 708-712, 1997.

[3] G. Box, G. Jenkins, and G. Reinsel, *Time Series Analysis Forecasting and Control*, 3rd Ed., Prentice Hall, New Jersey, 1994.

[4] J.T. Bingham, M. P. Schoen, "Characterization of Myoelectric Signals Using System Identification Techniques," 2004 ASME International Mechanical Engineering Congress and Exposition (IMECE 2004), Anaheim, CA, November 13-19, 2004.

[5] R. Tubiana, *Examination of Hand and Wrist*, 2nd edition, Martin Dunitz Ltd.,1996.

[6] V. Frankel et al., *Basic Biomechanics of the Muscoskeletal System*, 2nd edition, Lippincott Williams & Wilkins,1989.

[7] D. A. Winter, *Biomechanics and Motor Control of Human Movement*, 2nd edition, Wiley-Interscience, New York, 1990.

[8] S. Van Sint Jan, D.J. Guirintano, D.E. Thompson, and M. Rooze, "Joint Kinematics Simulation from Medical Imaging Data", IEEE Transactions on Biomedical Engineering, 44(12):1175-1180, 1997.

[9] L.W. Tsai, and B. Roth, "Design of Dyads with Helical, Cylindrical, Spherical, Revolute and Prismatic Joints," Mechanism and Machine Theory, 7:591-598, 1972.

[10] C.H. Suh, and C.W. Radcliffe, *Kinematics and Mechanisms Design*, John Wiley & Sons, New York, 1978.

[11] E. Lee, and C. Mavroidis, "Geometric Design of 3R Manipulators for Reaching Four End-Effector Spatial Poses," The International Journal of Robotics Research, 23(3): 247-254, 2004.

[12] A. Perez, and J.M. McCarthy, "Clifford Algebra Exponentials and Planar Linkage Synthesis Equations", ASME Journal of Mechanical Design, 127(5): 931-940, 2005.

[13] A. Perez, and J.M. McCarthy, "Sizing a Serial Chain to Fit a Task Trajectory Using Clifford Algebra Exponentials", 2005 IEEE International Conference on Robotics and Automation, Barcelona, April 18-22, 2005.

[14] J.M. Selig, *Geometrical Methods in Robotics*, Springer-Verlag, New York, 1996.

[15] M.C. Villa-Uriol, F. Kuester, N. Bagherzadeh, A. Perez, and J.M. McCarthy, J, "Kinematic Synthesis of Avatar Skeletons from Visual Data", Advances in Robot Kinematics, J. Lenarcic and C. Galletti, eds., Kluwer Academic Publishing, 2004.